

Owen Fracture Zone: the Arabia-India plate boundary unveiled

M. Fournier^{1,2,3*}, N. Chamot-Rooke³, M. Rodriguez^{1,2,3}, P. Huchon^{1,2}, C. Petit⁴, M.-O.
Beslier⁴, S. Zaragosi⁵

¹ iSTeP, UMR 7193, UPMC Université Paris 6, Case 129, 4 place Jussieu, F-75005 Paris, France

² iSTeP, UMR 7193, CNRS, F-75005 Paris, France

³ Laboratoire de Géologie, CNRS UMR 8538, Ecole normale supérieure, 24 rue Lhomond, F-75005
Paris, France

⁴ Géosciences Azur, CNRS UMR 6526, Observatoire océanologique, BP48, 06235 Villefranche-sur-mer,
France

⁵ EPOC, CNRS UMR 5805, Université Bordeaux 1, Avenue des Facultés, 33405 Talence, France

* Corresponding author: marc.fournier@upmc.fr

15 **Abstract.** We surveyed the Owen Fracture Zone at the boundary between the
16 Arabia and India plates in the NW Indian Ocean using a high-resolution multibeam
17 echo-sounder (Owen survey, 2009) for search of active faults. Bathymetric data
18 reveal a previously unrecognized submarine fault scarp system running for over
19 800 km between the Sheba Ridge in the Gulf of Aden and the Makran subduction
20 zone. The primary plate boundary structure is not the bathymetrically high Owen
21 Ridge, but is instead a series of clearly delineated strike-slip fault segments
22 separated by several releasing and restraining bends. Despite abundant sedimentary
23 supply by the Indus River flowing from the Himalaya, fault scarps are not obscured
24 by recent deposits and can be followed over hundreds of kilometres, pointing to very
25 active tectonics. The total strike-slip displacement of the fault system is 10-12 km,
26 indicating that it has been active for the past ~3 to 6 million years if its current rate
27 of motion of $3 \pm 1 \text{ mm year}^{-1}$ has remained stable. We describe the geometry of this
28 recent fault system, including a major pull-apart basin at the latitude 20°N , and we
29 show that it closely follows an arc of small circle centred on the Arabia-India pole of
30 rotation, as expected for a transform plate boundary.

31

31 **1. Introduction**

32 The Arabia-India plate motion is currently accommodated along the Owen
33 Fracture Zone (OFZ) in the NW Indian Ocean (Wilson, 1965; Matthews, 1966;
34 Whitmarsh, 1979; Gordon and DeMets, 1989). The OFZ belongs to the large strike-
35 slip plate boundaries like the San Andreas, Dead Sea, North Anatolian and Alpine
36 faults in the continental domain, and the Macquarie Ridge in the oceanic domain
37 (Mann, 2007; Weber et al., 2009; Stein et al., 1997; Le Pichon et al., 2005; Massel et
38 al., 2000; Lebrun et al., 2003). The OFZ is marked by a moderate seismicity and by a
39 prominent bathymetric ridge, the Owen Ridge, up to 2,000-m high with respect to
40 the surrounding seafloor (Fig. 1). The Owen Ridge acts as a barrier to turbidites of
41 the Indus deep-sea Fan and prevents their sedimentation towards the west into the
42 Owen Basin (Mountain and Prell, 1990; Clift et al., 2001). As indicated by dextral
43 strike-slip focal mechanisms of earthquakes along the OFZ (Quittmeyer and Kafka,
44 1984; Gordon and DeMets, 1989; Fournier et al., 2001), the Arabian plate moves
45 northwards slightly faster than the Indian plate at a differential rate of 2 to
46 4 mm year⁻¹ estimated independently from geodetic (Fournier et al., 2008b) and
47 geological (DeMets et al., 1990, 1994, 2010) data. We recently surveyed the OFZ
48 onboard the *R/V Beautemps-Beaupré* (Owen survey, 2009) using a high-resolution
49 deep-water multibeam echo-sounder and a 3.5 kHz sub-bottom seismic profiler to
50 identify surficial traces of active faults and characterize the geometry of the fault
51 system in relation with its kinematics. Magnetic and gravity measurements were also
52 routinely acquired.

53

54 **2. Geometry of the plate boundary**

55 Multibeam bathymetric data reveal an outstanding active submarine fault system
56 between the Beautemps-Beaupré Basin to the south (Fig. 1; Fournier et al., 2008a)
57 and the Dalrymple Trough to the north (Edwards et al., 2008). The fault scarps are
58 well preserved on the seafloor and run at the base of the east-facing escarpment of
59 the Owen Ridge, except at its southern extremity and in its central part where the
60 faults crosscut the ridge (Fig. 1). The fault system is remarkably linear and focused
61 on a single strand along much of its length. Six main fault segments can be
62 identified, apparently uninterrupted over lengths between 60 and 180 km (Fig. 2).
63 The overall geometry of the fault system hereafter described, including releasing and
64 restraining bends, pull-apart basins localized on releasing bends, and basins ending
65 the fault system, is consistent with a dextral strike-slip motion.

66 We used an oblique Mercator projection with the Arabia-India pole of rotation as
67 pole of projection to test if the trace of the OFZ follows a small circle of the Arabia-
68 India motion (Fig. 2a). In this coordinate system, transform faults should be
69 horizontal straight lines if they strictly follow small circles. The trace of the OFZ is
70 generally parallel to a small circle and is diverted from it between 16.5°N and
71 20.3°N, where a system of adjacent releasing and restraining bends constituting a
72 paired bend (Mann, 2007) is observed. The releasing bend is made up of two pull-
73 apart basins, a small rhomboidal basin at 18.6°N (see Fig. 1a) and a larger basin at a
74 change in trend of the OFZ at 20°N (see section 4). Between 16.5°N and 18°N, the
75 fault trace slightly deviates from the direction of the interplate slip vector, leading to
76 the development of a gentle restraining bend. Minor compressional structures
77 adjacent to the restraining bend are deduced from the seafloor morphology east of
78 the fault and from the observation of folds and reverse faults in the recent deposits

79 on 3.5 kHz profiles. At the northern end of the OFZ, a second restraining bend
80 associated with folds on the Indian plate side is observed.

81 To further test the transform motion of the OFZ, we determined the location of
82 the Arabia-India pole from the great circles perpendicular to the fault. As shown in
83 Figure 2b, the great circles perpendicular to the fault strike, measured out of
84 releasing or restraining bends, intersect close to the rotation pole independently
85 determined from GPS and seismicity data (Fournier et al., 2008b) , and close to the
86 best-fitting Arabia-India pole determined from geological data (fault azimuths;
87 DeMets et al., 2010). The closure-enforced MORVEL Arabia-India rotation pole
88 (DeMets et al., 2010), which is located much farther to the east (3.2°S , 116.6°E),
89 predicts right-lateral slip parallel to the OFZ between 15°N and 18.5°N , becoming
90 more and more extensional north of 18.5°N (Fig. 2a). Thus, recent kinematic models
91 agree that the present-day OFZ is a pure strike-slip plate boundary over ~ 400 km
92 between 15°N and 18.5°N and that, north of 18.5°N , the motion is dominantly
93 strike-slip, but a small component of boundary-normal extensional motion cannot be
94 excluded. MORVEL solution requires a partitioning mechanism north of 18.5°N to
95 accommodate the predicted extensional component of boundary-normal motion,
96 since segments 4 and 5 are pure strike-slip (Fig. 2a). On the other hand, MORVEL
97 prediction is pure strike-slip along segment 6, at the entrance of the Dalrymple
98 horsetail, whereas our model would imply a small component of compression. Non
99 strike-slip components, either extensional or compressional, are expected to be so
100 small that, if distributed over a wide area, they may be difficult to recognize.

101

102 **3. Age of the active fault system**

103 The active fault system crosscuts the Owen Ridge and offsets it dextrally. The
104 total displacement is well constrained between 10 and 12 km by two strike-slip
105 offsets of morphologic features (Fig. 1a and b). A long-term extrapolation of the
106 GPS-derived slip rate of the OFZ ($3 \pm 1 \text{ mm year}^{-1}$) would restore the observed offset
107 in ~ 3 to 6 million years. The small finite offset therefore testifies that the present-
108 day fault system initiated recently, most probably during the Pliocene.

109 The reconstruction of the Arabia-India plate motion from the Somalia-Arabia and
110 Somalia-India plate motion models (Merkouriev and DeMets, 2006; Fournier et al.,
111 2010), indicates that the OFZ rate of motion remained nearly stable since oceanic
112 spreading initiated in the Gulf of Aden 20 Ma ago (Chamot-Rooke et al., 2009). This
113 result implies that, before the development of the present-day fault system, the
114 Arabia-India motion was accommodated by an older fault system, or 'paleo OFZ',
115 inactive since ~ 3 -6 Ma.

116 The development of the present-day fault system postdates the uplift of the
117 southern and central parts of the Owen Ridge. The onset of uplift of the southern
118 Owen Ridge, related to vertical motions on the paleo OFZ (Weissel et al., 1992), is
119 recorded by the transition from turbidites to pelagic sediments and is precisely dated
120 by drilling of the Early Miocene (19 Ma; Whitmarsh et al., 1974; Shipboard Scientific
121 Party, 1989). The onset of uplift of the Owen Ridge is synchronous of the initiation of
122 seafloor spreading in the Gulf of Aden, constrained by the age of the oldest magnetic
123 anomaly identified (An 6, 19.7 Ma; Fournier et al., 2010).

124

125 **4. Tectonic record in the 20°N pull-apart basin**

126 The main releasing bend along the OFZ is marked by a 90-km-long pull-apart
127 basin at the latitude of 20°N (Fig. 3). The 20°N-Basin corresponds to a right

128 step-over of 12 km between two master strike-slip faults trending N25°E south of the
129 basin and N30°E north of it. The dimensions of the 20°N-Basin (90 x 12 km) are of
130 the same order than those of the Dead Sea pull-apart basin (132 x 16 km; Ten Brink
131 et al., 1993) along the Dead Sea strike-slip fault on the western side of the Arabian
132 plate. The 20°N-Basin becomes wider (25 km) and deeper (4050 m) to the north,
133 where it is bounded to the west by a master normal fault scarp with a vertical throw
134 of 500 m, and to the east by three normal fault scarps with throws between 100 and
135 300 m stepping down towards the basin axis (profile P2 in fig. 3).

136 The spindle shape of the 20°N-Basin can be compared to pull-apart basins of
137 sandbox analogue models formed in pure strike-slip or transtensional setting (Smit et
138 al., 2008; Wu et al., 2009). The overall geometry of the 20°N-Basin compares closely
139 with pull-aparts developed in pure strike-slip regime (Wu et al., 2009). In particular,
140 the 20°N-Basin does not exhibit margins of en-echelon oblique-extensional faults,
141 typical of transtensional basins. This observation further confirms that the OFZ is a
142 pure strike-slip feature.

143 The 20°N-Basin is directly supplied in turbidity-current deposits by an active
144 channel of the Indus Fan (the mouth of the Indus river is 800 km away towards the
145 northeast), which deeply incises the recent deposits (Fig. 3). The channel displays a
146 moderate sinuosity, compared with nearby highly meandering abandoned channels,
147 which attests of a resumption of erosion on a steeper gradient. Similar changes in
148 gradient are evidenced by abandoned channels, raised and tilted in the vicinity of the
149 active faults (Fig. 3), indicating local tectonic uplift provoked by the fault motion. The
150 trace of the active faults bounding the 20°N-Basin is not obscured by turbiditic
151 deposits despite the slow rate of slip of the OFZ. The preservation of normal fault
152 scarps bounding the basin indicates that the rate of vertical (dip-slip) motion along

153 the faults has exceeded the rate of deposition and burial by the sediments of the
154 Indus Fan. The tectonic process is therefore dominant over deposition.

155 Sub-bottom seismic profiles (3.5 kHz) across the 20°N-Basin show that the basin
156 is asymmetric with a turbidite sequence that becomes thicker towards the north,
157 where the present-day depocentre of the basin is located (profile P1 in fig. 3).
158 Turbiditic currents feeding the 20°N-Basin could be related to the regional seismicity
159 and/or to the activity of the Indus River in relation with sea-level variations. The
160 basin could thus preserve a record of the seismic activity of the OFZ in its sediments,
161 and possibly of the seismicity of the Makran subduction zone.

162

163 **5. Terminations of the Owen Fracture Zone**

164 At its both tips, the OFZ terminates into extensional structures associated with
165 basins. To the north, the OFZ ends into the Dalrymple Trough by a system of
166 regularly spaced normal faults that branch from the master strike-slip fault and form
167 a spectacular 30-km-wide horsetail splay (Fig. 4a). The normal faults delineate a
168 series of deep basins (up to 4000 m deep), which constitute the southern part of the
169 Dalrymple Trough. The horsetail splay is indicative of slip dying out gradually
170 towards the northern tip of the OFZ. To the south in contrast, the OFZ terminates
171 abruptly into the Beutemps-Beaupré Basin, a 50-km-wide and 120-km-long basin
172 bounded by two N70-N90°E-trending conjugate master normal faults (Fig. 4b;
173 Fournier et al., 2008a). The basin is characterized by a strong negative gravity
174 anomaly in relation with a thick sedimentary infill of at least 3-4 km. Recent works on
175 the Arabia-India-Somalia triple junction showed that the Arabia-India motion was
176 transferred to the west of the Beutemps-Beaupré Basin along a dextral shear zone,
177 which joins southward the Sheba Ridge axis (Fournier et al., 2010). Numerous

178 landslide scars are observed on the slopes of the Beautemps-Beaupré Basin and the
179 southern Owen Ridge (Fig. 4b and 4c). Giant landslides, probably triggered by
180 earthquakes along the active fault system, massively impinge the western flank of
181 the Owen Ridge and were evacuated westward in the Owen Basin. Because of their
182 huge volume, these mass failures represent a potential source of tsunami for the
183 nearby coasts of Oman (Okal et al., 2006; Donato et al., 2009).

184

185 **6. Conclusion**

186 Our work sheds light on a previously unknown 800-km-long active fault system
187 associated with giant landslides at the Arabia-India plate boundary. These results will
188 motivate a reappraisal of the seismic and tsunami hazard assessment in the NW
189 Indian Ocean (Okal and Synolakis, 2008; Heidarzadehet al., 2008a). We show that
190 the OFZ is a pure strike-slip boundary between the Arabian and Indian plates. The
191 geometry of the active fault system is probably controlled both by the pre-existing
192 faults of the paleo OFZ and by the topography of the Owen Ridge since the 20°N-
193 Basin is located at the main threshold of the ridge. Extrapolating the present-day slip
194 rate of the OFZ for 3-6 million years accounts for its total displacement. The initiation
195 of strike-slip motion along the present-day fault system does not coincide with any
196 tectonic event recorded onland in Oman (Lepvrier et al., 2002; Fournier et al., 2004,
197 2006), but is coeval with a major tectonic reorganization of the Arabia-Eurasia
198 collision from western Turkey to Iran between 3 and 7 Ma (Axen et al., 2001; Allen
199 et al., 2004; Shabanian et al., 2009) deduced from the extrapolation of short-term
200 deformation rates. It is also synchronous with the initiation of extrusion of Anatolia
201 ca. 5 Ma (Armijo et al., 1999) and the onset of seafloor spreading in the Red Sea 4-5
202 million years ago (Cochran and Karner, 2007). The lateral transport of the Anatolian

203 lithosphere out of the collision zone could be at the origin of this widespread
204 reorganization, including initiation of the present-day fault system at the Arabia-India
205 plate boundary.

206

207 **Acknowledgements.** We are indebted to the Captain Geoffroy de Kersauson,
208 officers, and crew members of the *BHO Beautemps-Beaupré*, and to the French Navy
209 hydrographers Vincent Lamarre and Yves-Marie Tanguy, and the hydrographic team
210 of the 'Groupe Océanographique de l'Atlantique', for their assistance in data
211 acquisition. We acknowledge the support of SHOM, IFREMER, and INSU-CNRS for
212 the Owen cruise. We thank Thierry Garlan from SHOM for making available
213 bathymetric data of the Fanindien survey. We also thank C. DeMets his insightful
214 review.

215

215 **Figure captions**

216

217 **Figure 1.** Active fault scarps of the OFZ mapped with a multibeam echo-sounder
218 can be followed over 800 km from the Beautemps-Beaupré Basin to the Dalrymple
219 Trough (white arrows). The OFZ is bounded to the east by the Indian plate oceanic
220 floor of Paleocene age formed at the Carlsberg Ridge (Chaubey et al., 2002; Royer et
221 al., 2002), overlain by thick deposits (up to 12 km) of the Indus Fan (the second
222 largest deep-sea fan), and to the west by the Owen Basin floored with oceanic crust
223 of poorly constrained age between Late Jurassic and Eocene (Whitmarsh, 1979;
224 Mountain and Prell, 1990; Edwards et al., 2000). The Owen Ridge is made up of
225 three distinct portions separated by two thresholds at 18.2°N and 20°N. The
226 southern ridge is asymmetric with a steep east-facing scarp and a gentle western
227 flank, whereas the central ridge displays a dome morphology elongated in the
228 direction of the Owen fracture zone. The southern and central ridges do not bear any
229 magnetic signal. In contrast, the northern ridge, which rises ~2500 m above the
230 surrounding seafloor and is topped by a flat platform at depths of 400 m below
231 present sea level, is characterized by high amplitude magnetic anomalies attesting of
232 a volcanic origin. It corresponds to the Qalhat Seamount, a volcanic guyot of
233 probable Cretaceous age like the Little Murray Ridge in the Oman Basin (Edwards et
234 al., 2000; Gaedicke et al., 2002; Ellouz-Zimmermann et al., 2007). a and b, Strike-
235 slip geomorphologic offsets of the active faults reach 10 to 12 km.

236

237 **Figure 2.** Two graphical tests confirm that the OFZ is a transform fault. a, On an
238 oblique Mercator map where the pole of projection has been shifted to the Arabia-
239 India rotation pole (12.1°N, 76.2°E; Fournier et al., 2008b), the OFZ is aligned with

240 Eulerian parallels (black dashed line), as expected for a transform fault. Between
241 16.5°N and 20.3°N, the fault trace is deviated from the horizontal reference line by a
242 paired bend, but returns to it once the bend is passed. A small circle about the
243 closure-enforced MORVEL Arabia-India rotation pole (blue dashed line; DeMets et al.,
244 2010) is parallel to an horizontal straight line south of 18.5°N and diverge
245 increasingly from it north of 18.5°N. Six apparently uninterrupted fault segments are
246 labelled from 1 to 6. b, Great circles perpendicular to the fault trace intersect near
247 the Arabia-India rotation pole (12.1°N, 76.2°E) shown by a red star with its 95%
248 confidence ellipse. The best-fitting MORVEL Arabia-India pole is shown by an open
249 circle (DeMets et al., 2010). The closure-enforced MORVEL Arabia-India pole (-3.2°N,
250 116.6°E) and the GPS-based Arabia-India pole of Reilinger et al. (2006; 17.7°N,
251 110.9°E) are located more than 30° toward the east.

252

253 **Figure 3.** The 20°N pull-apart basin is located at the main threshold of the Owen
254 Ridge, south of the Qalhat Seamount. The basin is directly supplied in turbiditic
255 deposits by an active channel of the Indus Fan. Two sub-bottom seismic profiles
256 across the basin, along (P1) and perpendicular (P2) to its great axis, show that the
257 turbiditic deposits, characterized on profiles by an alternation of thin highly reflective
258 levels and thick transparent layers, are tilted towards the north due to motion of the
259 border normal fault. White arrows indicate the master strike-slip faults.

260

261 **Figure 4.** a, The horsetail splay of the Dalrymple Trough developed in the northern
262 tip-damage zone of the OFZ. Normal faults branch from the master strike-slip fault at
263 low angles, curve progressively and become parallel to the maximum horizontal
264 stress. b, Giant submarine landslides, probably due to strong ground motions from

265 earthquakes of nearby active faults, occurred on western flank of the Owen Ridge
266 and are suspected to have generated tsunami (Heidarzadehet al., 2008b). c.
267 Perspective view from the northwest of a multi-events generated landslide and
268 related headwall collapses. This landslide removed up to 14 km³ of material from the
269 pelagic cover of the Owen Ridge (Rodriguez et al., submitted to Marine Geology).
270 Location in Figure 4b.
271

271 **References**

- 272 Allen, M., Jackson, J., Walker, R., 2004. Late Cenozoic reorganization of the Arabia-
273 Eurasia collision and the comparison of short-term and long-term deformation
274 rates. *Tectonics* 23, TC2008, doi:10.1029/2003TC00153.
- 275 Armijo, R., Meyer, B., Hubert-Ferrari, A., Barka, A.A., 1999. Propagation of the North
276 Anatolian fault into the northern Aegean: Timing and kinematics. *Geology* 27,
277 267-270.
- 278 Axen, G.J., Lam, P.S., Grove, M., Stockli, D.F., Hassanzadeh, J., 2001. Exhumation of
279 the west-central Alborz Mountains, Iran, Caspian subsidence, and collision-related
280 tectonics. *Geology* 29 (6), 559–562.
- 281 Chamot-Rooke, N., Fournier, M., Scientific Team of AOC and OWEN cruises, 2009.
282 Tracking Arabia-India motion from Miocene to Present, American Geophysical
283 Union, Fall Meeting 2009.
- 284 Chaubey, A. K, Dymant, J., Bhattacharya, G. C., Royer, J.-Y., Srinivas, K., Yattheesh,
285 V., 2002. Paleogene magnetic isochrons and paleo-propagators in the Arabian and
286 Eastern Somali basins, Northwest Indian Ocean. In: P. Clift, D. Kroon, C. Gaedicke
287 and J. Craig (eds), *The Tectonic and Climatic Evolution of the Arabian Sea Region*.
288 *Geological Society Special Publication, 195*, 71-85.
- 289 Clift, P.D., Shimizu, N., Layne, G.D., Blusztain, J.S., Gaedicke, C., Schluter, H.U.,
290 Clark, M.K., Amjad, S., 2001. Development of the Indus Fan and its significance
291 for the erosional history of the Western Himalaya and Karakoram. *Geol. Soc. Am.*
292 *Bull.* 113 (8), 1039–1051.
- 293 Cochran, J.R., Karner, G. D., 2007. Constraints on the deformation and rupturing of
294 continental lithosphere of the Red Sea: The transition from rifting to drifting, in

295 The Origin and Evolution of the Caribbean Plate, in James, K.H., Lorente, M.A.,
296 Pindell J.L. (Eds.), *Geol. Soc. Spec. Pub.*, 282, 265–289, doi:10.1144/SP282.13.

297 DeMets, C., Gordon, R.G., Argus, D.F., 2010. Geologically current plate motions.
298 *Geophys. J. Int.* 181, 1-80, doi: 10.1111/j.1365-246X.2009.04491.x

299 DeMets, C., Gordon, R.G., Argus, D.F., Stein, S., 1990. Current plate motions.
300 *Geophys. J. Int.* 101, 425-478.

301 DeMets, C., Gordon, R.G., Argus, D.F., Stein, S., 1994. Effect of recent revisions of
302 the geomagnetic reversal time scale on estimates of current plate motions.
303 *Geophys. Res. Lett.* 21, 2191-2194.

304 Donato, S.V., Reinhardt, E.G., Boyce, J.I., Pilarczyk, J.E., Jupp, B.P., 2009. Particle-
305 size distribution of inferred tsunami deposits in Sur Lagoon, Sultanate of Oman.
306 *Mar. Geol.* 257, 54-64.

307 Edwards, R.A., Minshull, T.A., Flueh, E.R., Kopp, C., 2008. Dalrymple Trough: An
308 active oblique-slip ocean-continent boundary in the northwest Indian Ocean. *Earth*
309 *Planet. Sci. Lett.* 272, 437-445.

310 Edwards, R.A., Minshull, T.A., White, R.S., 2000. Extension across the Indian–
311 Arabian plate boundary: the Murray Ridge. *Geophys. J. Int.* 142, 461-477.

312 Ellouz-Zimmermann, N., et al., 2007. Offshore frontal part of the Makran
313 Accretionary prism: The Chamak survey (Pakistan). In: Lacombe, O., Lavé, J.,
314 Roure, F., Vergés, J. (Eds.). *Thrust Belts and Foreland Basins - From Fold*
315 *Kinematics to Hydrocarbon System*, *Frontiers in Earth Science Series*, Springer
316 Berlin Heidelberg, 351-366.

317 Fournier, M., Bellahsen, N., Fabbri, O., Gunnell, Y., 2004. Oblique rifting and
318 segmentation of the NE Gulf of Aden passive margin. *Geochem. Geophys.*
319 *Geosyst.* 5, Q11005, doi:10.1029/2004GC000731.

320 Fournier, M., Chamot-Rooke, N., Petit, C., Fabbri, O., Huchon, P., Maillot, B.,
321 Lepvrier, C., 2008b. In-situ evidence for dextral active motion at the Arabia-India
322 plate boundary. *Nature Geoscience* 1, 54-58, doi:10.1038/ngeo.2007.24

323 Fournier, M., Chamot-Rooke, N., Petit, C., Huchon, P., Al-Kathiri, A., Audin, L.,
324 Beslier, M.O., d'Acromont, E., Fabbri, O., Fleury, J.M., Khanbari, K., Lepvrier, C.,
325 Leroy, S., Maillot, B., Merkouriev, S., 2010. Arabia-Somalia plate kinematics,
326 evolution of the Aden-Owen-Carlsberg triple junction, and opening of the Gulf of
327 Aden. *J. Geophys. Res.* 115, B04102, doi:10.1029/2008JB006257

328 Fournier, M., Lepvrier, C., Razin, P., Jolivet L., 2006. Late Cretaceous to Paleogene
329 post-obduction extension and subsequent Neogene compression in the Oman
330 Mountains. *GeoArabia* 11, 17-40.

331 Fournier, M., Patriat, P., Leroy, S., 2001. Reappraisal of the Arabia-India-Somalia
332 triple junction kinematics. *Earth Planet. Sci. Lett.* 189, 103-114.

333 Fournier, M., Petit, C., Chamot-Rooke, N., Fabbri, O., Huchon, P., Maillot, B.,
334 Lepvrier, C., 2008a. Do ridge-ridge-fault triple junctions exist on Earth? Evidence
335 from the Aden-Owen-Carlsberg junction in the NW Indian Ocean. *Basin Research*
336 20, 575-590, doi: 10.1111/j.1365-2117.2008.00356.x

337 Gaedicke, C., Prexl, A., Schlüter, H.U., Meyer, H., Roeser, H., Clift, P., 2002. Seismic
338 stratigraphy and correlation of major regional unconformities in the northern
339 Arabian Sea. In: Clift, P.D., Kroon, D., Gaedicke, C., Craig, J. (Eds.), *The Tectonic
340 and Climatic Evolution of the Arabian Sea Region. : Special Publications* 195.
341 Geological Society, London, pp. 25–36.

342 Gordon, R.G., DeMets, C., 1989. Present-day motion along the Owen fracture zone
343 and Dalrymple trough in the Arabian Sea. *J. Geophys. Res.* 94, 5560-5570.

344 Heidarzadeh, M., Pirooz, M.D., Zaker, N.H., Yalciner, A.C., 2008a. Preliminary
345 estimation of the tsunami hazards associated with the Makran subduction zone at
346 the northwestern Indian Ocean. *Nat. Hazards*. doi:10.1007/s11069-008-9259-x.

347 Heidarzadeh, M., Pirooz, M.D., Zaker, N.H., Yalciner, A.C., Mokhtari, M., Esmaeily, A.,
348 2008b. Historical tsunami in the Makran Subduction Zone off the southern coasts
349 of Iran and Pakistan and results of numerical modeling. *Ocean Eng.* 35, 774–786.

350 Le Pichon X., Kreemer, C., Chamot-Rooke, N., 2005. Asymmetry in elastic properties
351 and the evolution of large continental strike-slip faults, *J. Geophys. Res.* 110,
352 B03405, doi : 10.1029/2004JB003343.

353 Lebrun, J.-F., Lamarche, G., Collot, J.-Y., 2003. Subduction initiation at a strike-slip
354 plate boundary: the Cenozoic Pacific-Australian plate boundary, south of New
355 Zealand. *J. Geophys. Res.* 108, B9, 2453, doi:10.1029/2002JB002041.

356 Lepvrier, C., Fournier, M., Bérard, T., Roger, J., 2002. Cenozoic extension in coastal
357 Dhofar (southern Oman): Implications on the oblique rifting of the gulf of Aden.
358 *Tectonophysics*, 357, 279-293.

359 Mann, P., 2007. Global catalogue, classification and tectonic origins of restraining-
360 and releasing bends on active and ancient strike-slip fault systems. *Geol. Soc.*
361 *London Spec. Pub.*, 290, 13-142.

362 Massell, C., Coffin, M.F., Mann, P., Mosher, S., Frohlich, C., Schuur, C.L., Karner,
363 G.D., Ramsay, D., Lebrun, J.F., 2000. Neotectonics of the Macquarie ridge
364 complex, Australia-Pacific plate boundary. *J. Geophys. Res.* 105, 13457-13480.

365 Matthews, D.H., 1966. The Owen fracture zone and the northern end of the
366 Carlsberg Ridge. *Phil. Trans. Royal Soc. A*, 259, 172-186.

367 Merkuriev, S., DeMets, C., 2006. Constraints on Indian plate motion since 20 Ma
368 from dense Russian magnetic data: Implications for Indian plate dynamics.
369 *Geochem. Geophys. Geosyst.* 7, Q02002, doi:10.1029/2005GC001079.

370 Mountain, G.S., Prell, W.L., 1990. A multiphase plate tectonic history of the
371 southeast continental margin of Oman, in: Robertson, A.H.F., Searle, M.P., Ries,
372 A.C. (Eds), *The Geology and Tectonics of the Oman Region*, Geol. Soc. London
373 *Spec. Pub.*, 49, 725-743.

374 Okal, E.A., Fritz, H.M., Raad, P.E., Synolakis, C.E., Al-Shijbi, Y., Al-Saifi, M., 2006.
375 Oman field survey after the December 2004 Indian Ocean tsunami. *Earthquake*
376 *Spectra* 22 (S3), S203–S218.

377 Okal, E.A., Synolakis, C.E., 2008. Far-field tsunami hazard from mega-thrust
378 earthquakes in the Indian Ocean. *Geophys. J. Int.* 172, 995–1015.

379 Quittmeyer, R. C., Kafka, A. L., 1984. Constraints on plate motions in southern
380 Pakistan and the northern Arabian Sea from the focal mechanisms of small
381 earthquakes. *J. Geophys. Res.* 89, 2444-2458.

382 Reilinger R. et al., 2006. GPS constraints on continental deformation in the Africa-
383 Arabia-Eurasia continental collision zone and implications for the dynamics of plate
384 interactions. *J. Geophys. Res.* 111, B05411, doi:10.1029/2005JB004051.

385 Rodriguez, M., Fournier, M., Chamot-Rooke, N., Huchon, P., Zaragosi, S., Rabaute,
386 A. Mass wasting processes along the Owen fracture zone (Northwest Indian
387 Ocean), *submitted to Marine Geology*.

388 Royer, J.-Y., Chaubey, A.K., Dymant, J., Bhattacharya, G.C., Srinivas, K., Yatheesh,
389 V., Ramprasad, T., 2002. Paleogene plate tectonic evolution of the Arabian and
390 Eastern Somali basins. In: *The Tectonic and Climatic Evolution of the Arabian Sea*

391 Region (Ed. by P. Clift, D. Kroon, C. Gaedicke and J. Craig), Geol. Soc. Spec. Pub.,
392 195, 7-23.

393 Shabanian, E., Siame, L., Bellier, O., Benedetti, L., Abbassi, M.R., 2009. Quaternary
394 slip rates along the northeastern boundary of the Arabia–Eurasia collision zone
395 (Kopeh Dagh Mountains, Northeast Iran). *Geophys. J. Int.* 178, 1055-1077, doi:
396 10.1111/j.1365-246X.2009.04183.x

397 Shipboard Scientific Party, 1989. Site 731. In Prell, W.L., Niitsuma, N., et al., Proc.
398 ODP, Init. Repts., 117: College Station, TX (Ocean Drilling Program), 585-652.

399 Smit, J., Brun, J.P., Cloetingh, S., Ben-Avraham, Z., 2008. Pull-apart basin formation
400 and development in narrow transform zones with application to the Dead Sea
401 Basin. *Tectonics* 27. doi:10.1029/2007TC002119.

402 Stein, R. S., Barka, A. A., Dieterich, J. H., 1997. Progressive failure of the North
403 Anatolian Fault since 1939 by earthquake stress triggering. *Geophys. J. Int.* 128,
404 594–604, doi:10.1111/j.1365-246X.1997.tb05321.x.

405 Ten Brink, U.S., Ben-Avraham, Z., Bell, R.E., Hassouneh, M., Coleman, D.F.,
406 Andreasen, G., Tibor, G., Coakley, B., 1993. Structure of the Dead Sea pull-apart
407 basin from gravity analyses. *J. Geophys. Res.* 98 (B12), 21,877-21,894,
408 doi:10.1029/93JB02025

409 Weber, M., et al., 2009. Anatomy of the Dead Sea Transform from lithospheric to
410 microscopic scale. *Rev. Geophys.* 47, RG2002, doi:10.1029/2008RG000264.

411 Weissel, J.K., Childers, V.A., Karner, G.D., 1992. Extensional and Compressional
412 Deformation of the Lithosphere in the Light of ODP Drilling in the Indian Ocean.
413 Synthesis of Results from Scientific Drilling in the Indian Ocean, Geophysical
414 Monography 70, American Geophysical Union.

415 Whitmarsh, R.B., 1979. The Owen Basin off the south-east margin of Arabia and the
416 evolution of the Owen Fracture Zone. *Geophys. J. Royal Astron. Soc.* 58, 441-470.
417 Whitmarsh, R.B., Weser, O.E., Ross, D.A. & al., 1974. Initial report DSDP, U.S.
418 Government Printing Office, Washington, D.C., v. 23, p. 1180.
419 Wilson, T. J., 1965. A new class of faults and their bearing on continental drift.
420 *Nature* 207, 343-347.
421 Wu, J. E., McClay, K., Whitehouse, P., Dooley, T., 2009. 4D analogue modelling of
422 transtensional pull-apart basins. *Mar. Petr. Geol.* 26, 1608-1623.

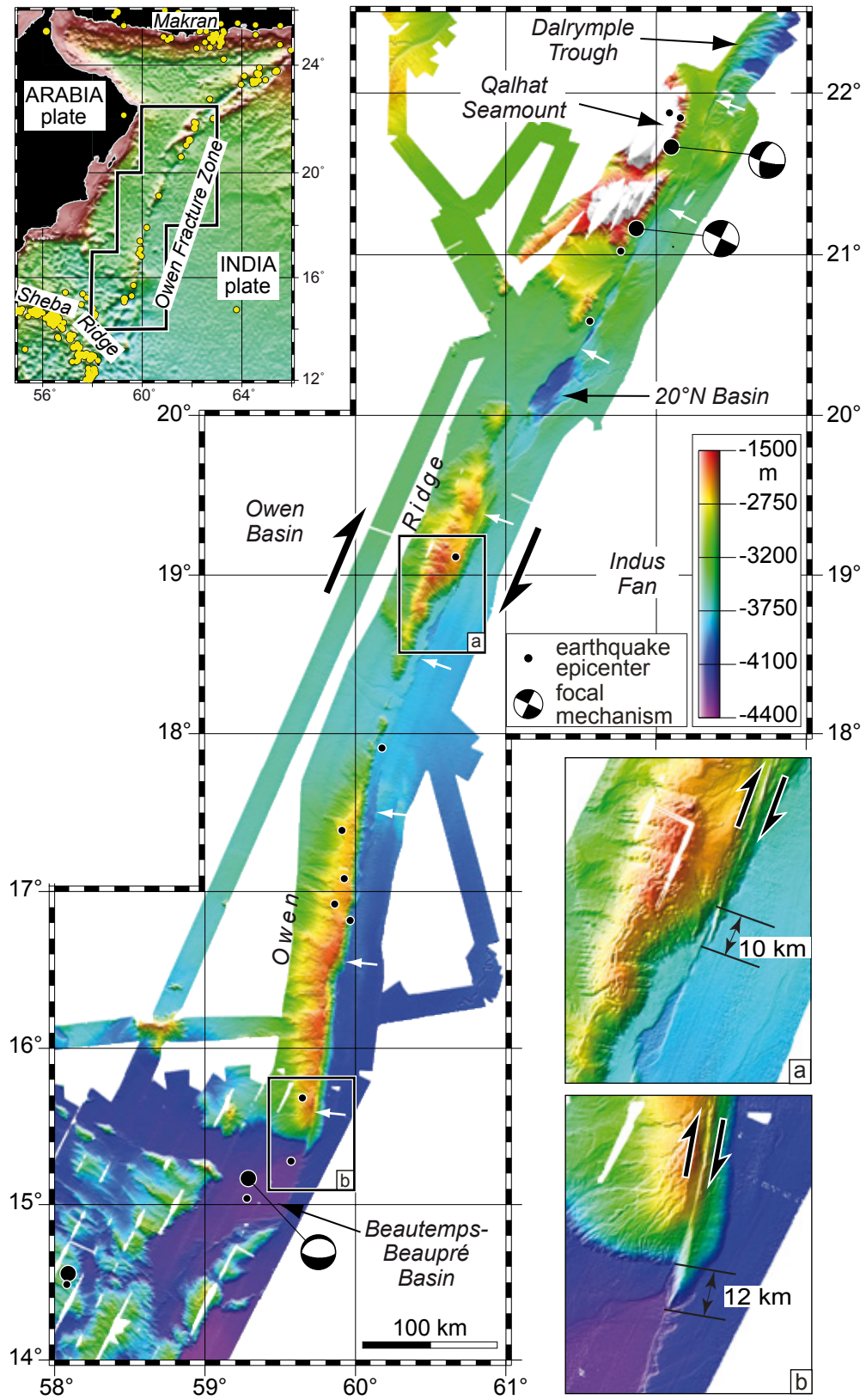


Figure 1

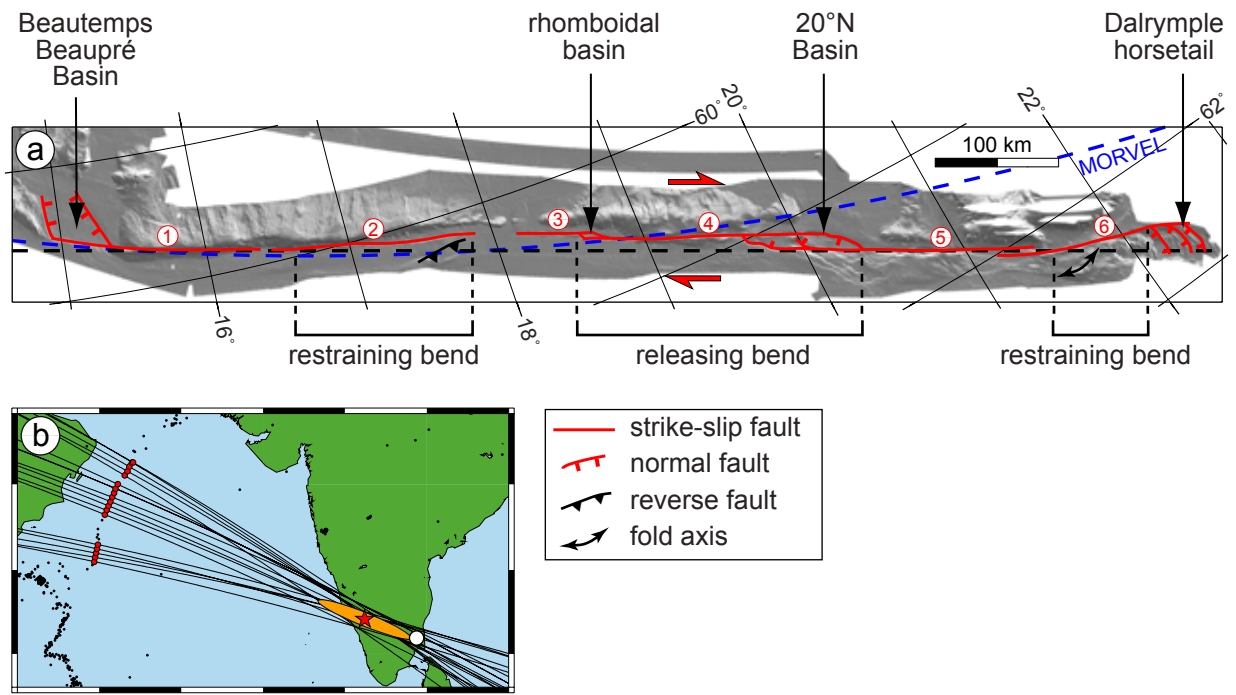


Figure 2

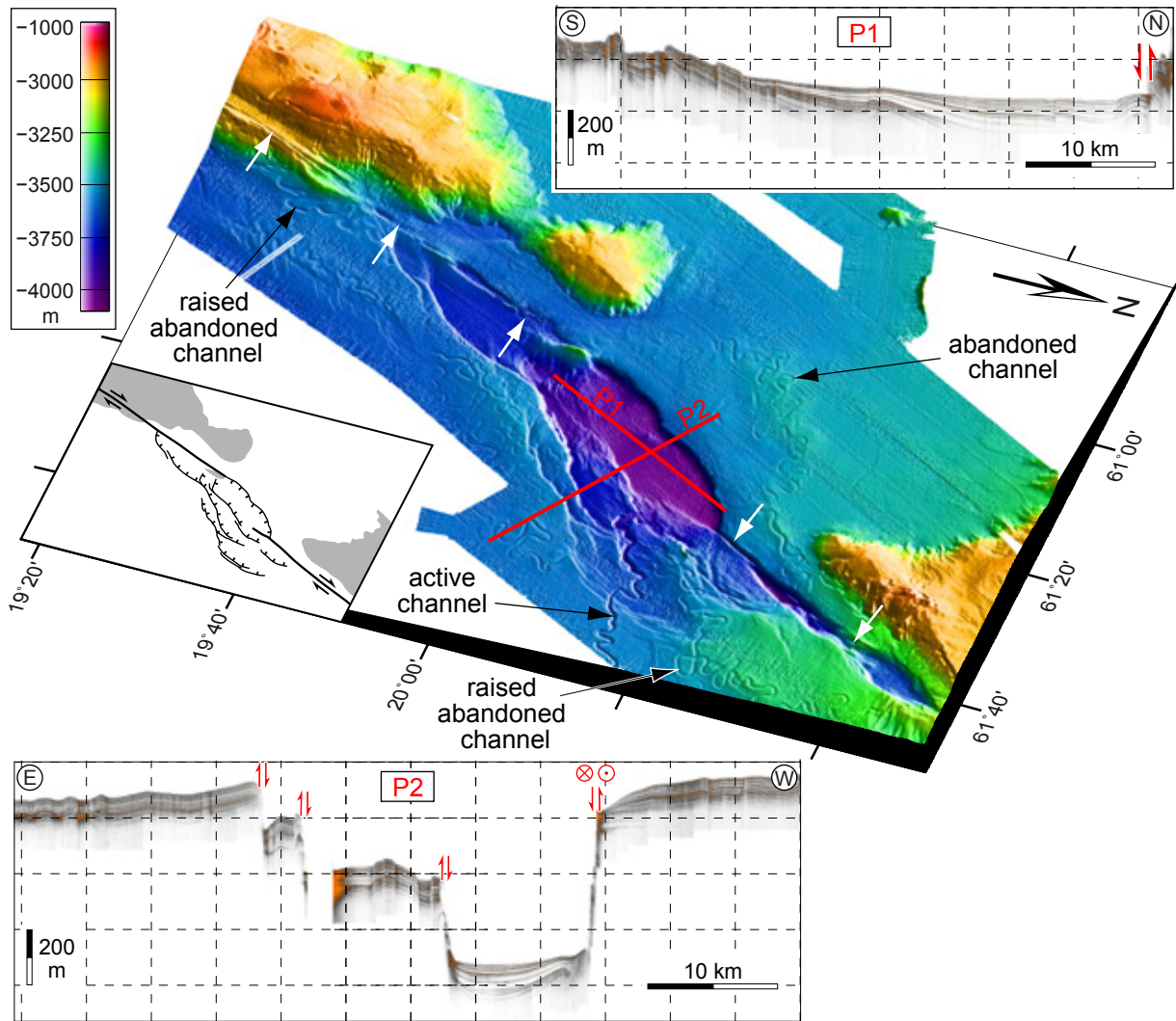


Figure 3

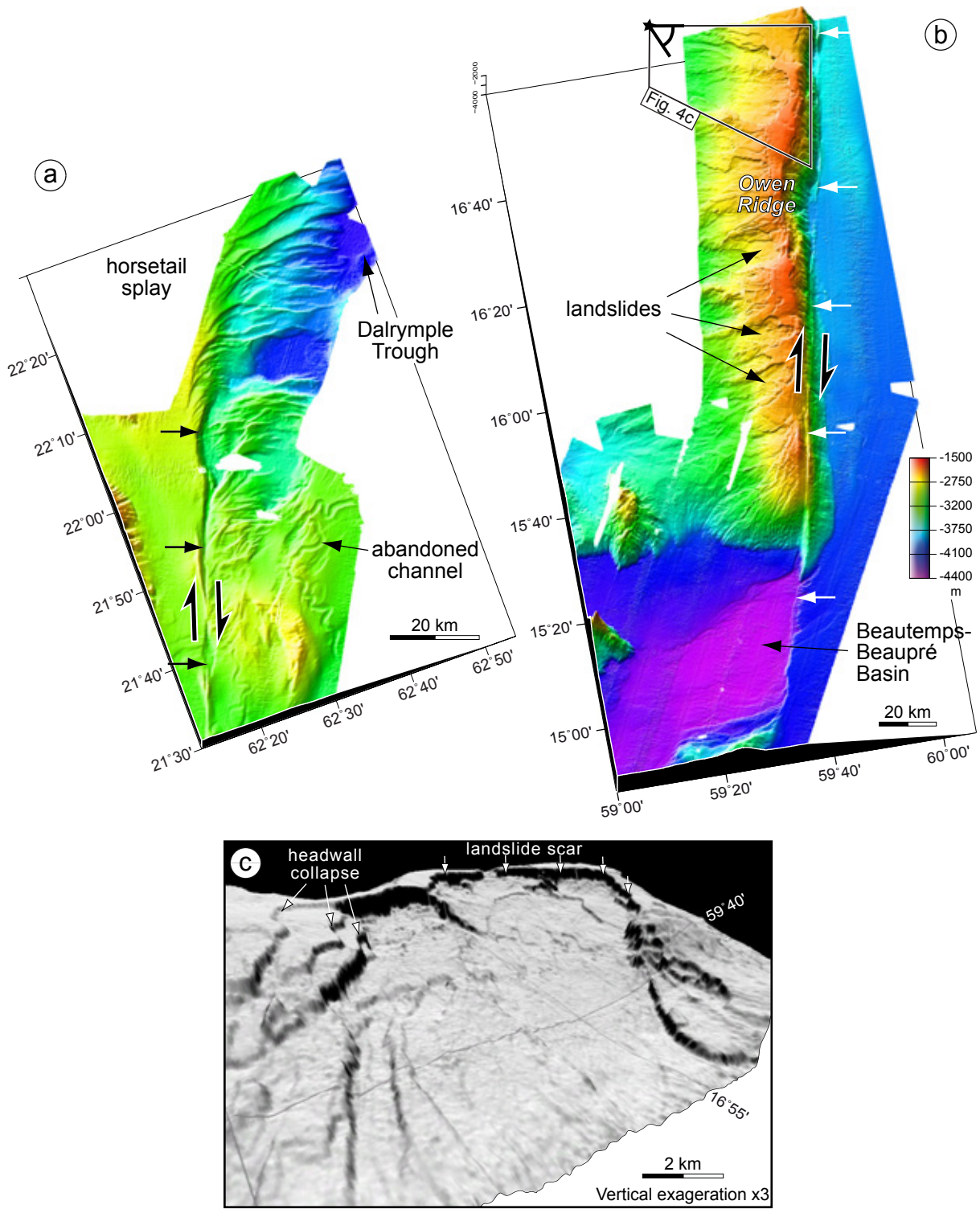


Figure 4